Chemistry & Biology, Vol. 11, 991–998, July, 2004, ©2004 Elsevier Ltd. All rights reserved. DOI 10.1016/j.chembiol.2004.05.010

Quantum Chemical Calculations and Mutational Analysis Suggest Heat Shock Protein 90 Catalyzes *Trans-Cis* Isomerization of Geldanamycin

Yong-Sok Lee,[1,*] Monica G. Marcu,[2] and Len Neckers[2]
[1]Center for Molecular Modeling
Center for Information Technology
National Institutes of Health
Building 12A, Room 2049
Bethesda, Maryland 20892
[2]Urologic Oncology Branch
Center for Cancer Research
National Cancer Institute
Rockville, Maryland 20850

Summary

The affinity of geldanamycin (GA) for binding to heat shock protein 90 (HSP90) is 50- to 100-fold weaker than is the affinity of the structurally distinct natural product radicicol. X-ray crystallography shows that although radicicol maintains its free conformation when bound to HSP90, the conformation of GA is dramatically altered from an extended conformation with a *trans* amide bond to a kinked shape in which the amide group in the ansa ring has the *cis* configuration. We have performed ab initio quantum chemical calculations to demonstrate that the *trans-cis* isomeriztion of GA in solution is both kinetically and thermodynamically unfavorable. Thus, we propose that HSP90 catalyzes the isomerization of GA. We identify Ser113, a conserved residue outside the ATP binding pocket, as essential for the isomerization of GA. In support of this model, we show that radicicol binds equally well to both wild-type HSP90 and the Ser113 mutant, whereas the binding of GA to the Ser113 mutant is decreased significantly from its binding to wild-type HSP90. Based on this finding, a mechanism of keto-enol tautomerization of GA catalyzed by HSP90 is proposed. The added requirement of isomerization prior to tight binding may explain the enhanced binding affinity of GA for HSP90 in a cell extract versus in a purified form.

Introduction

Radicicol (Figure 1A) and geldanamycin (GA, Figure 1B) are structurally distinct antibiotics that specifically bind to an amino-terminal nucleotide pocket in the molecular chaperone heat shock protein 90 (HSP90) [1–4]. Drug binding inhibits the chaperone's ability to stabilize a host of client proteins, many of which cancer cells use to promote their survival in toxic environments [5]. Recent X-ray crystallographic structures of HSP90 complexed with either radicicol [6] or GA [7, 8] have spurred great interest in designing inhibitors of HSP90 with enhanced potency and specificity [9].

Understanding the binding mechanics of these small molecules is important for rational design of novel HSP90 inhibitors, and the binding process, particularly in the case of GA, is not as simple as it may appear. For example, although the affinity of GA for purified HSP90 is approximately 1 μM in vitro [6], its apparent affinity in a cell extract is in the low nanomolar range [10, 11]. This is in distinct contrast to radicicol, which has a similar low nanomolar affinity for HSP90 both in its purified form and in a cellular milieu [6, 12]. Furthermore, a synthetic molecule based on a purine scaffold binds with micromolar affinity to both purified and cellular HSP90 [9].

Although the X-ray structure shows that the conformation of radicicol bound to the ATP/ADP binding site of HSP90 is identical to that of unbound radicicol [6], the conformation of GA bound to HSP90 is significantly different from that of unbound GA. GA bound to HSP90 adopts a compact conformation in which the benzoquinone and ansa rings are parallel to each other and resemble a C-clamp-like structure, whereas unbound GA preferentially adopts an extended conformation [7, 8]. The difference in conformation between bound and unbound GA has been attributed to the loss of coplanarity between the amide group and the benzoquinone in the compact conformation as well as to differences in solvents used during crystallization.

Examination of the X-ray structure of bound GA indicates that the amide group bonded to the benzoquinone has a *cis* (Figure 1C) configuration. This is in direct contrast with the X-ray structures of unbound ansamycins such as GA [13], herbimycin [14], and macbecin [15], which all show the same amide group in a *trans* configuration. The fact that the dihedral angle, C20-N22-C1-O, of bound GA (−165°) is significantly different from that of unbound GA (8°), herbimycin (−9°), or macbecin (8°) further supports that GA bound to HSP90 exists in the *cis* configuration.

Based on targeted molecular-dynamics simulations (TMD) of a GA derivative, 17-desmethoxy-17-N-N-dimethylaminoethylaminogeldanamycin (17-DMAG), Jez et al. have recently pointed out that 17-DMAG needs to undergo both macrocyclic ring conformational change and *trans-cis* isomerization of the amide in order to bind to HSP90 [16]. By assuming that the bound 17-DMAG has the *cis* amide configuration, this work studied the structural change of 17-DMAG by using molecular-mechanics force-field analysis to transform the *trans* amide to the *cis* form. This TMD study has provided insight into the process of *trans-cis* isomerization of 17-DMAG within the scope of a molecular-mechanics approximation. Although rotation of the C-N bond faces a substantial energy barrier of approximately 20 kcal/mol [17, 18], as well as a rearrangement of π electrons, the TMD study has not considered the energy barrier for the isomerization of the amide bond. Therefore, this process needs to be examined at a higher level of quantum chemistry, i.e., the approach needs to go beyond molecular mechanics. In addition, the TMD study has assumed

*Correspondence: leeys@mail.nih.gov

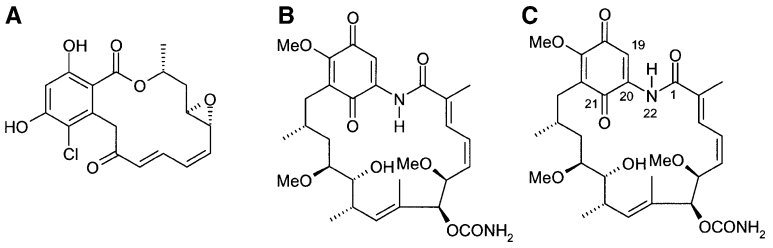

Figure 1. Chemical structures of radicicol and GA

(A) Radicicol.
(B) *Trans*-GA.
(C) *Cis*-GA.

that *trans-cis* isomerization of 17-DMAG occurs spontaneously without participation of HSP90.

In the present work, we have carried out *ab-initio* quantum chemical calculations on both free and bound GA to compare their geometry and energetics. We also constructed the reaction path of the *trans-cis* isomerization of GA by rotating the C20-N22 and C1-N22 bond of GA (Figure 1C). We then combined these calculations with the study of site-directed mutagenesis of HSP90 to identify the amino acid residue likely to be involved in the isomerization of GA. Based on these findings, a mechanism for the *trans-cis* isomerization of GA as well as a rationale for the enhanced binding affinity of GA for HSP90 in a cell extract is given.

Results and Discussion

Geometry and Energetics

The geometry-optimized structures of extended *trans*-GA and compact *cis*-GA are illustrated in Figures 2A and 2B, respectively. The optimized conformations of both closely resemble their respective starting X-ray structures. For example, the superposition of heavy atoms of the optimized *cis*-GA onto bound GA gives a root mean square deviation of 0.51 Å. Both optimized structures have a longer C1-N22 amide bond distance (1.39 Å for *trans* and 1.41 Å for *cis*) coupled with a shorter C20-N22 distance (1.37 Å for *trans* and 1.39 Å for *cis*). These bond distances indicate that the lone pair of electrons on the amide nitrogen is delocalized over the C20 atom of the quinone and the C1 atom of the amide group.

Table 1 lists the energetics of GA at 298.5 K in the gaseous phase. These values are essentially identical to those values calculated in DMSO, suggesting that solvent effects are negligible. The extended *trans*-GA conformation in DMSO is 13.8 kcal/mol more stable than the *cis*-GA in a compact conformation. When the entropy contribution is included, the free-energy difference between the two isomers increases to 15.5 kcal/mol because the *cis*-GA in a compact conformation has a slightly lower entropy than the extended *trans*-GA. These energetics clearly demonstrate that virtually all GA (>99.9999999%) exists in an extended *trans* configuration, explaining why the reported X-ray structures of unbound ansamycins have depicted only the *trans* configuration. In addition, preliminary NMR analysis has shown only a single broad resonance for the amide hydrogen of GA at milimolar concentration in DMSO (Barchi et al., unpublished data). Previous NMR evaluation of GA in $CDCl_3$ has also reported only a single species [19]. These NMR findings are consistent with the thermodynamic calculation reported here that equilibrium in solvent greatly favors *trans*-GA ($K_{eq} > 10^{11}$).

Trans-cis Isomerization of GA

Rigid docking studies of GA to HSP90 indicate that extended *trans*-GA cannot be fitted into the active site. To adopt the conformation of bound *cis*-GA, the extended *trans*-GA in solution must undergo flipping of the ansa ring over the benzoquinone as well as *trans-cis* isomerization of the amide bond. The flipping of the ansa ring can occur readily as evidenced by the X-ray structures of ansamycins, which have shown that the ansa ring can be positioned on either side of the benzoquinone. However, the *trans-cis* isomerization involves a breaking of the C-N amide bond, which requires a substantial energy because of its partial double-bond character. The question is then whether this *trans-cis* isomerization occurs spontaneously or is assisted by residues of HSP90. The spontaneous process in solution can be ruled out because the conversion of *trans* to *cis* GA is thermodynamically unfavorable by 15.5 kcal/mol (Table 1) irrespective of the rotational energy barrier of the C-N bond. Therefore, we hypothesize that HSP90 lowers the energy barrier for the isomerization of GA, and the resulting *cis*-GA is subsequently stabilized by interaction with the residues of HSP90 as observed in the X-ray structures. To explore this hypothesis, we individually mutated Lys112 and Ser113 residues of HSP90 to alanine and examined the ability of the resultant point mutants to bind to immobilized GA and to immobilized ATP. These particular residues were chosen based on docking of the optimized extended *trans*-GA outside the binding pocket of GA. As illustrated in Figure 3, the side chain of both Lys112 and Ser113 of HSP90 can H-bond with the amide oxygen of *trans*-GA, and this may facilitate the *trans-cis* isomerization process. Ser113 is an ideal candidate for this role not only because of its strict conservation among HSP90 family members but also because it is located where the putative isomerization would have to occur, outside of the nucleotide binding pocket.

Mutational Analysis of HSP90 Binding to Immobilized GA and ATP

As shown in Figure 4A (left panel), binding of GA to the S113A HSP90 point mutant was markedly impaired. GA binding to the K112A mutant was also reduced in comparison to wild-type HSP90. The published X-ray structure of GA bound to HSP90 shows that Lys112 forms an H-bond with the quinone oxygen of GA (Figure 3) at the solvent-exposed entrance to the nucleotide binding pocket [7]. The K112A mutant may display partially im-

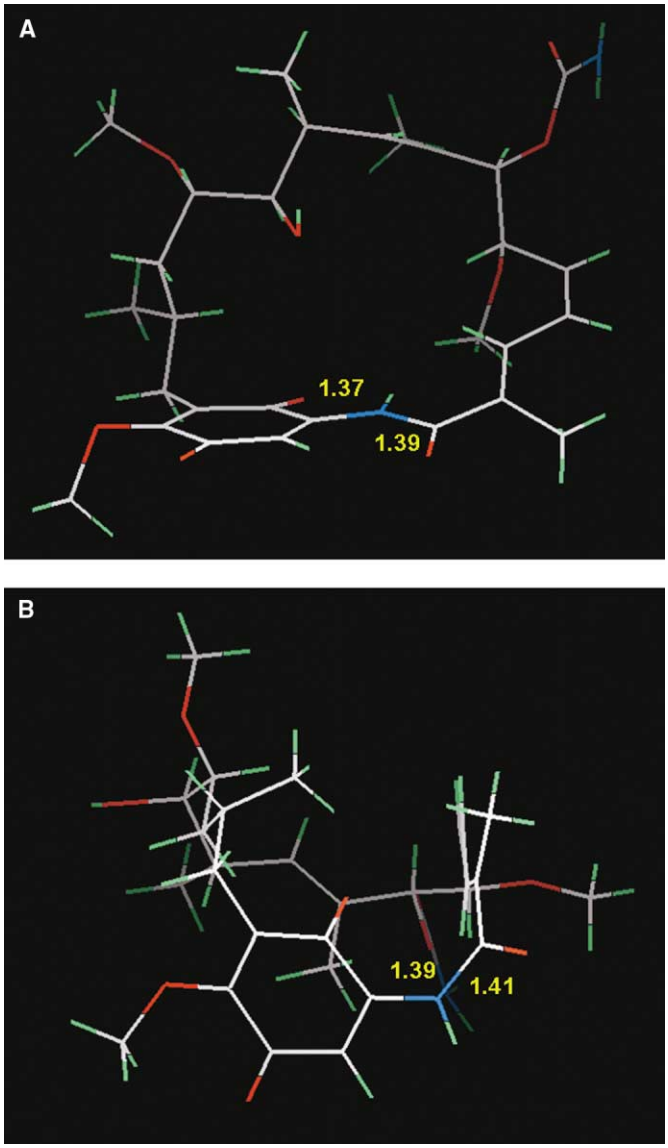

Figure 2. *Ab Initio* Energy-Minimized Structures of GA

(A) Extended *trans*-GA.

(B) Compact *cis*-GA. Atoms represented by colors: white, carbon; green, hydrogen; blue, nitrogen; and red, oxygen.

paired GA binding as a result of the loss of this H-bonding interaction. However, the X-ray structure does not provide an obvious structural basis for the dramatic impairment of GA binding by the S113A mutant. In fact, the X-ray structure shows that Ser113 is not positioned to interact directly or indirectly with either GA or radicicol.

Figure 4B demonstrates that although GA has difficulty displacing the S113A mutant from ATP beads, radicicol is as effective in this regard as it is toward displacing wild-type HSP90. These data indicate strongly that S113 is involved in the initial binding of *trans*-GA to HSP90 prior to its isomerization. Although it is possible that a conformational change in the S113A mutant prevents GA from entering the pocket, it is difficult to reconcile this speculation with the fact that the binding of the more structurally rigid radicicol is not affected by this mutation. Based on a recent study [20] that used computational modeling to link the individual X-ray structures of the N-terminal and middle domains of HSP90, it could be argued that GA would not have access to S113 in the context of the complete protein. This model was based on the assumption that the conformation of HSP90 can be inferred by homology from crystallographic data obtained from Gyrase B and MutI, two other ATP binding proteins that share similar nucleotide binding site topology with HSP90. However, this assumption is highly speculative because neither GA nor radicicol bind to either Gyrase B or MutI proteins (Neckers et al., unpublished observations). Thus, the homology between these three proteins is clearly not sufficient

Table 1. Relative Energetics of Geldanamycin (kcal/mol) at 298.5 K

	B3LYP/6-31G* Enthalpy	Gibbs Free energy
extended *trans*-GA	0	0
compact *cis*-GA	13.3 (13.8)[a]	14.9(15.5)[a]

[a]Single point energy calculation in DMSO with the Onsager method [29]

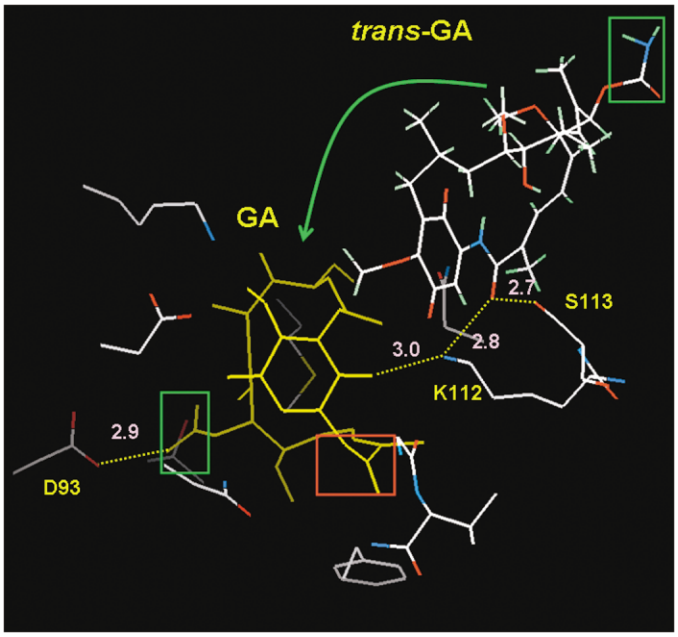

Figure 3. Proposed Binding Site of *trans*-GA

Bound GA (1a4h) H-bonded to Asp93 and Lys112 is shown in yellow. The red box indicates the *cis*-amide group of the bound GA; the green box indicates the carbamate group of both *trans* and bound GA. The optimized *trans*-GA was docked to H-bond with Lys112 and Ser113; the Ser113 oxygen was steered to H-bond with the amide oxygen. *Trans*-GA is likely to undergo *trans-cis* isomerization with the assistance of Lys112 and Ser113 which, in turn, results in a flipping of the ansa ring. The green arrow indicates, schematically, a possible pathway through which GA could enter the binding pocket after the isomerization.

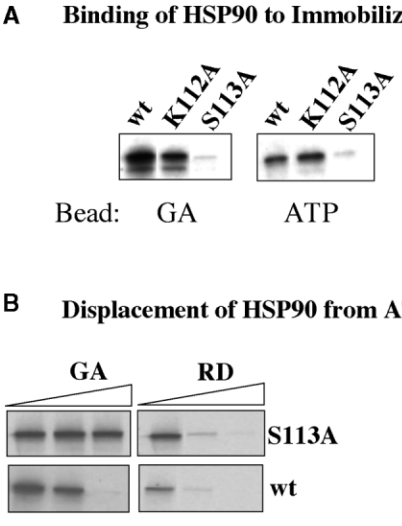

Figure 4. Binding Characteristics of Wild-Type and Point-Mutated HSP90 to GA and ATP

(A) Binding of wild-type and mutated HSP90 to immobilized GA and ATP resins. [^{35}S]methionine-labeled wild-type HSP90 and the K112A and S113A mutants were prepared by in vitro translation and tested for binding to either GA resin or ATP resin, as described in the Experimental Procedures. The amount of HSP90 added to the beads was normalized based on efficiency of translation. Bound HSP90 was eluted from the beads by being boiled in denaturing-gel loading buffer, and samples were separated by polyacrylamide gel electrophoresis. Gels were dried and exposed to X-ray film for 1–2 days. (B) Displacement of wild-type and S113A HSP90 from ATP-Sepharose beads. Radiolabeled HSP90 was prepared as above and incubated with ATP-Sepharose beads. In this experiment, three times as much S113A-containing lysate (compared to wild-type HSP90-containing lysate) was used, and film was exposed for 7 days in order to detect S113A binding to ATP beads. Increasing concentrations (0, 10, 100 nM) of GA and radicicol (RD) were added to the translated HSP90 30 min prior to addition of ATP beads, and samples were rotated at 4°C. Bound HSP90 was eluted and processed as above.

to allow one to correctly predict whether the proposed *trans*-GA binding site in the N-terminal domain of HSP90 is sterically hindered in the complete protein. Furthermore, it is very unlikely that the proposed *trans*-GA binding site overlaps with the middle segment of HSP90 because it is adjacent to the ATP binding pocket as shown in Figure 3.

Proposed Mechanism for *trans-cis* isomerization of GA

To investigate the putative *trans-cis* isomerization process, we rotated the C1-N22 amide bond of the *trans*-GA by varying the dihedral angle of H-N22-C1-O from −170° to 0° in increments of 10° while relaxing the rest of structure. The calculated energy barrier to rotation about this amide bond is 12.4 kcal/mol. Although the extended GA at the dihedral angle of 0° has the *cis* configuration (Figure 5), the amide hydrogen has an orientation that is almost opposite to that of the compact *cis*-GA (Figure 2B). This suggests that the C20-N22 bond of the *trans*-GA also needs to be rotated in order for the molecule to adopt the conformation of bound GA. Figure 6 illustrates that the potential energy of GA goes up as the dihedral angle of H-N22-C20-C21 increases from 0° to 90°. After passing the transition

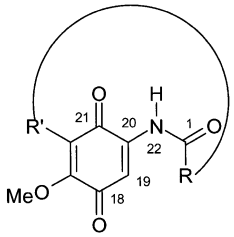

Figure 5. Schematic Representation of the Extended *cis*-GA. R and R′ indicate the portion of the ansa ring of GA

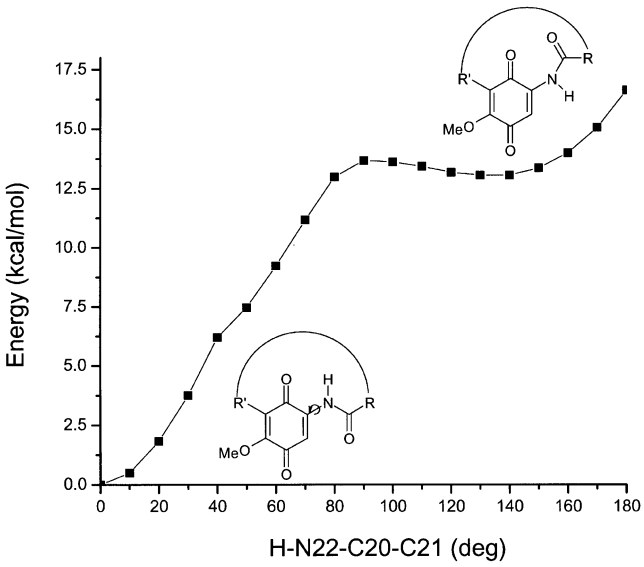

Figure 6. Plot of the Potential Energy of *trans*-GA versus the Dihedral Angle of H-N22-C20-C21

state, the potential energy remains rather flat until the dihedral angle reaches 170°. The calculated rotational energy barrier of the C20-N22 bond is 13.7 kcal/mol, which is 1.3 kcal/mol higher than that of the C1-N22 amide bond and is in good agreement with the fact that the C20-N22 bond distance is 0.02 Å shorter than the C1-N22 bond. This strongly suggests that the rotation of the C20-N22 bond is a rate-determining step for the isomerization of GA, thus making the *trans-cis* isomerization of the amide bond of secondary importance.

Due to extensive computational requirements, the overall energy barrier for *trans-cis* isomerization of GA was not calculated. Nonetheless, judging from the thermodynamic stability of *trans*-GA (15.5 kcal/mol) as compared to *cis*-GA and the sizable rotational energy barrier of the C20-N22 and C1-N22 bonds, the overall energy barrier for the isomerization of GA is expected to be well in excess of 20 kcal/mol, making the process also kinetically unfavorable. Unlike in solution, the thermodynamic instability of the compact *cis*-GA could be overcome by interaction energies provided by residues of HSP90 in the ATP binding pocket. However, in order for GA to interact with HSP90, both the C20-N22 and C1-N22 bonds of *trans*-GA must first be rotated.

Although it is not clear a priori how HSP90 lowers the rotational energy barriers, one possibility is that Ser113 plays mainly a structural role in docking the *trans*-GA near to the binding pocket. After docking, the rotation of both C20-N22 and C1-N22 bonds as well as the flipping of the ansa ring over the benzoquinone may somehow transform the *trans*-GA to the compact *cis*-GA, for example by an induced fit. The resulting conformation change would allow Asp93 at the bottom of the ATP binding pocket to steer the carbamate group of *cis*-GA into the binding pocket, presumably via electrostatic interaction (Figure 3). However, an induced fit by HSP90 alone is highly unlikely to provide sufficient energy to overcome the rotational barrier for the C20-N22 and C1-N22 bonds, which have a partial double bond character, and this makes the uncatalyzed conversion of *trans*-GA to *cis*-GA untenable, even in the vicinity of the ATP binding pocket of HSP90.

An alternative, more plausible rationale is that the isomerization of GA occurs through keto-enol tautomerization assisted by Lys112 and Ser113 as depicted in Figure 7. Because the amide hydrogen, like the imine hydrogen of the hydantoin ring, is very acidic, GA can exist as keto-enol tautomers. **A** and **D** depict *trans*- and *cis*-GA, respectively. Upon deprotonation of the amide hydrogen of **A**, an enol (**B**) can be formed by abstraction of a proton from Lys112. As a consequence, the C20-N22 bond of **B** can rotate readily. **C** is another enol formed by the proton transfer from the protonated Lys112 to the quinone oxygen atom. This enolization makes the amide C1-N22 bond of **C** also rotatable. As a consequence of the rotation of both C20-N22 and C1-N22 bonds, the *cis*-GA (**D**) results when the nitrogen atom of **C** is reprotonated. The reported H-bond between the quinone oxygen of GA and Lys112 (Figure 3) is likely to arise from this keto-enol tautomerization, in which Lys112 promotes the tautomerization by providing a proton to shuttle between the quinone and amide oxygen atoms while Ser113 binds to the amide oxygen of GA for initial docking and then assists the direction of rotation from *trans* to *cis*. In the absence of Lys112, the proton shuttling is likely to be carried out by a protonated water molecule. This may explain how the K112A mutant can still bind GA, albeit with reduced efficiency.

Interestingly, we found that, when compared to the K112A mutant or to wild-type HSP90 (Figure 4A, right panel), the S113A mutant bound poorly to ATP resin. ATP may exist in a number of orientations, but only one is likely to enter the pocket. Superposition of ADP to GA [6] shows that the amide group of GA and the α-phosphate group of ADP overlap well, as evidenced by the fact that the P_α atom of the phosphate and the C1 atom of the amide group are only separated by 0.4 Å. This suggests that Lys112 and Ser113 may also H-bond with the α-phosphate group of ATP. By this H-bonding interaction, Ser113 may act as a gatekeeper by permitting only a particular conformer of ATP to enter the HSP90 binding pocket.

Because of its thermodynamic instability, it should only be possible to detect *cis*-GA when it is bound to

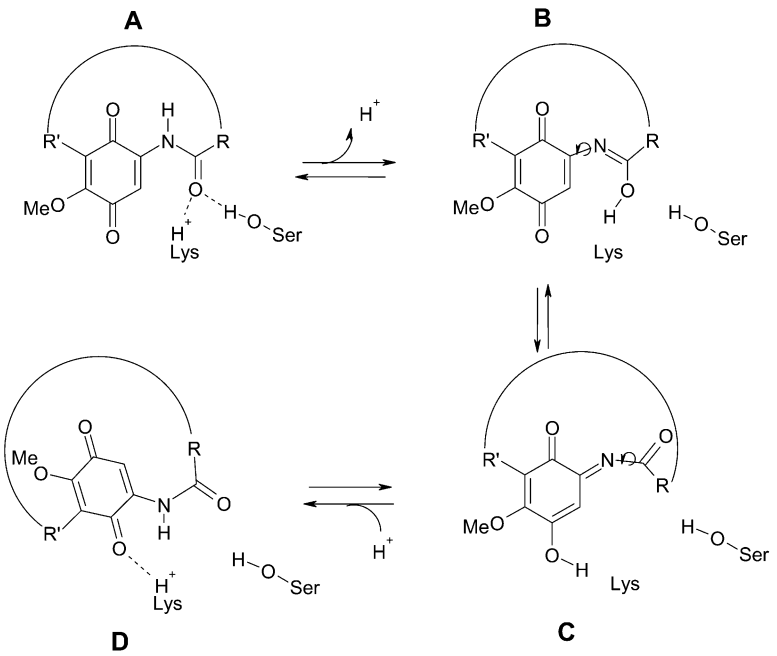

Figure 7. Schematic Representation of the GA *trans-cis* Isomerization Catalyzed by Lys112 and Ser113 of HSP90

A and **D** depict *trans*- and *cis*-GA, respectively. Upon deprotonation of the amide hydrogen of **A**, an enol (**B**) can be formed by abstraction of a proton from Lys112. As a consequence, the C20-N22 bond of **B** can be rotated readily. **C** is another enol form that allows the rotation of the C20-N22 bond. The *cis*-GA (**D**) results when the nitrogen atom of **C** is reprotonated upon the rotation of the C1-N22 bond and the flipping of the ansa ring. In this scheme, Lys112 promotes a keto-enol tautomerization by providing a proton to shuttle between the quinone and amide oxygen atoms, whereas Ser113 binds to the amide oxygen of GA for initial docking and then assists the direction of rotation from *trans* to *cis*.

HSP90. The vibrational frequency calculations suggest that the bending modes of N-H of *trans*- and *cis*-GA are significantly different both in frequency and intensity (details will be published elsewhere). Thus using these bending frequencies as a marker, one can use FT-IR differential spectroscopy to investigate the process of GA *trans-cis* isomerization mediated by HSP90. This will yield a spectroscopic identification of *cis*-GA aside from the X-ray structures.

HSP90 recognizes misfolded proteins and participates in their refolding in concert with other molecular chaperones [21]. These misfolded proteins may contain some *cis* peptide bonds. Whether the HSP90-dependent isomerization of GA is catalyzed by a motif in the chaperone that helps rectify misfolded proteins via *cis-trans* isomerization of their peptide bonds remains to be seen. Nonetheless, this possibility finds support in a recent NMR study demonstrating *cis-trans* isomerization of non-prolyl-containing peptides by HSP70 [22]. Does HSP90 view GA as a misfolded protein? Intriguingly, one of the original cocrystallization studies documenting GA binding to HSP90 speculated that the drug was recognized by the chaperone as a peptide mimetic [7]. Although this interpretation of the function of the GA binding pocket was eventually proven to be incorrect, Ser113 is not in the nucleotide pocket, and its involvement in an uncharacterized but spatially related peptide binding domain remains a possibility. Indeed, an N-terminal peptide binding site in HSP90 and its endoplasmic reticulum-localized homolog GRP94 has been described [23–25]. Furthermore, GA and ATP have been shown to decrease the peptide binding affinity of the N-terminal site while stimulating the release of already associated peptide [23, 24]. In contrast, both radicicol and peptide can bind simultaneously to the N-terminal domain of GRP94 [25].

These data may also help explain the fact that, in contrast to radicicol, whose HSP90 binding affinity is uniformly in the low nanomolar range, the binding affinity of GA for purified HSP90 is approximately 1 μM, whereas in a cell extract its affinity is increased 50- to 100-fold. In cells, HSP90 is associated with a number of cochaperone proteins that modify its activity [26]. Indeed, a recent study has demonstrated that the affinity of purified HSP90 for GA is dramatically improved upon addition of purified cochaperone proteins to the binding assay [27]. The possibility exists that one or more associated cochaperones further facilitates HSP90-dependent isomerization of *trans*-GA to *cis*-GA, perhaps by providing a basic residue to abstract the amide hydrogen and thereby enhancing apparent affinity. Another possibility is that one or more of these cochaperones might help trap *cis*-GA so that it can be drawn into the ATP binding pocket more readily. Because radicicol requires no isomerization to bind to HSP90, its affinity does not depend on the presence of cochaperones or other cellular factors.

Significance

Quantum chemical calculations have demonstrated that free GA exists in a *trans* configuration in solution. Because *trans*-to-*cis* isomerization is thermodynamically unfavorable by 15.5 kcal/mol, it is highly likely that HSP90 itself catalyzes the process. Based on the loss of GA binding to a Ser113 point mutant, it appears that the Ser113 residue of HSP90 is essential for promoting isomerization of *trans*-GA to *cis*-GA. We propose that HSP90 catalyzes the isomerization of GA through keto-enol tautomerization assisted by Lys112 and Ser113. The enhanced affinity of HSP90 for GA upon addition of purified cochaperone proteins may arise from further facilitation of HSP90-dependent isomerization of *trans*-GA to *cis*-GA by one or more

cochaperones, perhaps by providing a basic residue to abstract the amide hydrogen. HSP90 is an important molecular target in cancer, and its inhibition may prove to be a viable, novel approach to cancer therapy. Therefore, understanding the binding mechanics of these small molecules is important for rational design of improved HSP90 inhibitors.

Experimental Procedures

Quantum Chemical Calculation

The geometries of GA were optimized with density functional theory at the B3LYP/6-31G* level [28]. The extended *trans*-GA obtained from the Cambridge Structural Database [13] was modified to have a methoxy group at the C17 position. The compact GA bound to HSP90 (1a4h of the Protein Data Bank) was treated as having a *cis* ansa ring amide bond. In addition, the stereochemistry of C14 of the bound GA was corrected from the *S* to *R* configuration. Because DMSO was used to dissolve GA for binding assay measurements, single-point energy calculations on the geometry-optimized GAs were performed with the Onsager method [29] with the dielectric constant of DMSO taken to be 46.7. We calculated the rotational barrier for the C20-N22 and C22-N1 bond by varying a torsional angle in increments of 10° around the C20-N22 or C1-N22 bond while optimizing all other geometrical variables. No thermal energy and solvent effects were taken into account in estimating rotational barriers because of the computational cost.

HSP90 Mutation and Binding to GA and ATP Resins

Full-length, wild-type, chicken HSP90β cDNA (amino acids 1–728) subcloned in pGEM-7Z (Promega Corporation, Madison, WI) was a gift of Dr. David Toft (Mayo Clinic, Rochester, MN). This plasmid was the starting material for mutagenesis. A single amino acid (Lys112 or Ser 113 in the human sequence) was changed to Ala with the GeneEditor In Vitro Site-Directed Mutagenesis System (Promega Corporation). A mutagenesis primer was designed based on the cDNA sequence of HSP90 in the targeted region, and the second primer was included with the GeneEditor kit. After serial antibiotic selection, the mutants were isolated, and their sequences were confirmed by dideoxy sequencing.

In Vitro Transcription and Translation

Wild-type and mutant HSP90 were expressed from 1 μg of the respective plasmids by in vitro transcription/translation with the TNT rabbit reticulocyte lysate kit (Promega Corporation) in the presence of translation grade [^{35}S]methionine (1458 Ci/mmol, ICN, Costa Mesa, CA), with the appropriate DNA polymerase according to the manufacturer's instructions. Aliquots of in vitro translation reactions (1 μl) were checked for translation efficiency, and 1–3 μl were diluted in the appropriate buffer and incubated with either GA affinity beads or ATP-Sepharose (Upstate Biotechnology, Inc., Lake Placid, NY). Binding assays and visualization of bound HSP90 were performed as previously described [12]. GA affinity beads were prepared as previously described [4]. In the experiment shown in Figure 4B, 1 μl of wild-type HSP90 translation mix and 3 μl of the Ser113 mutant translation mix were used in order to obtain a detectable signal for the bound Ser113 mutant. Furthermore, the film depicting Ser113 binding in Figure 4B was exposed for 7 days (in comparison to a 1–2 day exposure to obtain the data shown in Figure 4A and the wild-type binding shown in Figure 4B).

Acknowledgments

We are indebted to Dr. Katsumi Sugiyama for providing insight into the proposed keto-enol tautomerization of GA catalyzed by HSP90. Useful discussions with Dr. Peter Steinbach and Dr. Sergio Hassan are acknowledged. This study utilized the high-performance computational capabilities of the Helix Systems at the National Institutes of Health, Bethesda, MD (http://helix.nih.gov).

Received: January 8, 2004
Revised: May 4, 2004
Accepted: May 6, 2004
Published: July 23, 2004

References

1. Grenert, J.P., Sullivan, W.P., Fadden, P., Haystead, T., Clark, J., Mimnaugh, E., Krutzsch, H., Ochel, H.J., Schulte, T.W., Sausville, E., et al. (1997). The amino-terminal domain of heat shock protein 90 (HSP90) that binds geldanamycin is an ATP/ADP switch domain that regulates HSP90 conformation. J. Biol. Chem. *272*, 23843–23850.
2. Schulte, T.W., Akinaga, S., Soga, S., Sullivan, W., Stensgard, B., Toft, D., and Neckers, L.M. (1998). Antibiotic radicicol binds to the N-terminal domain of HSP90 and shares important biologic activities with geldanamycin. Cell Stress Chaperones *3*, 100–108.
3. Sharma, S.V., Agatsuma, T., and Nakano, H. (1998). Targeting of the protein chaperone, HSP90, by the transformation suppressing agent, radicicol. Oncogene *16*, 2639–2645.
4. Whitesell, L., Mimnaugh, E.G., De Costa, B., Myers, C.E., and Neckers, L.M. (1994). Inhibition of heat shock protein HSP90-pp60v-src heteroprotein complex formation by benzoquinone ansamycins: essential role for stress proteins in oncogenic transformation. Proc. Natl. Acad. Sci. USA *91*, 8324–8328.
5. Isaacs, J.S., Xu, W., and Neckers, L. (2003). Heat shock protein 90 as a molecular target for cancer therapeutics. Cancer Cell *3*, 213–217.
6. Roe, S.M., Prodromou, C., O'Brien, R., Ladbury, J.E., Piper, P.W., and Pearl, L.H. (1999). Structural basis for inhibition of the HSP90 molecular chaperone by the antitumor antibiotics radicicol and geldanamycin. J. Med. Chem. *42*, 260–266.
7. Stebbins, C.E., Russo, A.A., Schneider, C., Rosen, N., Hartl, F.U., and Pavletich, N.P. (1997). Crystal structure of an HSP90-geldanamycin complex: targeting of a protein chaperone by an antitumor agent. Cell *89*, 239–250.
8. Prodromou, C., Roe, S.M., O'Brien, R., Ladbury, J.E., Piper, P.W., and Pearl, L.H. (1997). Identification and structural characterization of the ATP/ADP-binding site in the HSP90 molecular chaperone. Cell *90*, 65–75.
9. Chiosis, G., Timaul, M.N., Lucas, B., Munster, P.N., Zheng, F.F., Sepp-Lorenzino, L., and Rosen, N. (2001). A small molecule designed to bind to the adenine nucleotide pocket of HSP90 causes Her2 degradation and the growth arrest and differentiation of breast cancer cells. Chem. Biol. *8*, 289–299.
10. Schulte, T.W., and Neckers, L.M. (1998). The benzoquinone ansamycin 17-allylamino-17-demethoxygeldanamycin binds to HSP90 and shares important biologic activities with geldanamycin. Cancer Chemother. Pharmacol. *42*, 273–279.
11. Chiosis, G., Huezo, H., Rosen, N., Mimnaugh, E., Whitesell, L., and Neckers, L. (2003). 17AAG: Low target binding affinity and potent cell activity—finding an explanation. Mol. Cancer Ther. *2*, 123–129.
12. Schulte, T.W., Akinaga, S., Murakata, T., Agatsuma, T., Sugimoto, S., Nakano, H., Lee, Y.S., Simen, B.B., Argon, Y., Felts, S., et al. (1999). Interaction of radicicol with members of the heat shock protein 90 family of molecular chaperones. Mol. Endocrinol. *13*, 1435–1448.
13. Schnur, R., and Corman, M. (1994). Tandem [3,3]-sigmatropic rearrangements in an ansamycin: Stereospecific conversion of an (*S*)-allylic alcohol to an (*S*)-allylic amine derivative. J. Org. Chem. *59*, 2581–2584.
14. Furusaki, A., Matsumoto, T., Nakagawa, A., and Omura, S. (1980). Herbimycin A: an ansamycin antibiotic; X-ray crystal structure. J. Antibiot. (Tokyo) *33*, 781–782.
15. Muroi, M., Haibara, K., Asai, M., Kamiya, K., and Kishi, T. (1981). The structures of macbecin I and II: new tumor antibiotics. Tetrahedron *37*, 1123–1130.
16. Jez, J.M., Chen, J.C., Rastelli, G., Stroud, R.M., and Santi, D.V. (2003). Crystal Structure and Molecular Modeling of 17-DMAG in Complex with Human HSP90. Chem. Biol. *10*, 361–368.
17. Ilieva, S., Hadjieva, B., and Galabov, B. (2002). Theory supplemented by experiment. Electronic effects on the rotational stability of the amide group in p-substituted acetalinides. J. Org. Chem. *67*, 6210–6215.

18. Fischer, G. (2000). Chemical aspects of peptide bond isomerization. Chem. Soc. Rev. *29*, 119–127.
19. Andrus, M.B., Meredith, E.L., Simmons, B.L., Soma-Sekhar, B.B., and Hicken, E.J. (2002). Total synthesis of (+)-geldanamycin and (−)-o-quinogeldanamycin with use of asymmetric anti- and syn-glycolate aldol reactions. Org. Lett. *4*, 3549–3552.
20. Meyer, P., Prodromou, C., Hu, B., Vaughan, C., Roe, S.M., Panaretou, B., Piper, P.W., and Pearl, L.H. (2003). Mol. Cell *11*, 647–658.
21. Walter, S., and Buchner, J. (2002). Molecular chaperones–cellular machines for protein folding. Angew. Chem. Int. Ed. Engl. *41*, 1098–1113.
22. Scheine-Fischer, C., Habazettl, J., Schmid, F., and Fischer, G. (2002). The hsp70 chaperone DnaK is a secondary amide peptide bond cis-trans isomerase. Nat. Struct. Biol. *9*, 419–424.
23. Scheibel, T., Weikl, T., and Buchner, J. (1998). Two chaperone sites in HSP90 differing in substrate specificity and ATP dependence. Proc. Natl. Acad. Sci. USA *95*, 1495–1499.
24. Young, J.C., Schneider, C., and Hartl, F.U. (1997). In vitro evidence that HSP90 contains two independent chaperone sites. FEBS Lett. *418*, 139–143.
25. Vogen, S., Gidalevitz, T., Biswas, C., Simen, B.B., Stein, E., Gulmen, F., and Argon, Y. (2002). Radicicol-sensitive peptide binding to the N-terminal portion of GRP94. J. Biol. Chem. *277*, 40742–40750.
26. Pearl, L.H., and Prodromou, C. (2000). Structure and in vivo function of HSP90. Curr. Opin. Struct. Biol. *10*, 46–51.
27. Kamal, A., Thao, L., Sensintaffar, J., Zhang, L., Boehm, M.F., Fritz, L.C., and Burrows, F.J. (2003). A high-affinity conformation of HSP90 confers tumour selectivity on HSP90 inhibitors. Nature *425*, 407–410.
28. Frisch, M.J., Trucks, G.W., Schlegel, H.B., Scuseria, G.E., Robb, M.A., Cheeseman, J. A. Montgomery, J.A. Jr., Vreven, T., Kudin, K.N., et al. (2003). Gaussian *03*, Revision B.03. (Pittsburgh, PA: Gaussian, Inc).
29. Onsager, L. (1938). Electric moments of molecules in liquids. J. Am. Chem. Soc. *58*, 1486–1493.